ψ' Polarization due to color-octet quarkonia production

Adam K. Leibovich

Lauritsen Laboratory

California Institute of Technology

Pasadena, CA 91125

(February 1, 2008)

Abstract

We calculated the polarization of ψ' due to $gg \to Q\bar{Q}[^3P_J^{(8)}]g \to \psi^{(\lambda)}$ color-octet quarkonia production. We find that at low transverse momenta the ψ' is unpolarized due to the contributions proportional to the $L = S = 0$ and $L = S = 1$ color-octet matrix elements. As $p_\perp$ increases, the ψ' mesons become 100% polarized, as predicted by fragmentation calculations. Polarization due to lowest order color-singlet production is also considered, which qualitatively has a similar shape to the color-octet production.

14.40.Gx,13.87.Fh

Typeset using REVTEX

The study of quarkonia production has recently received renewed attention due to new data and interesting theoretical developments. Traditionally, quarkonia production has been calculated in the color-singlet model (CSM), where the heavy quark-antiquark pair is produced in a color-singlet configuration at distance scales short compared to Λ_{QCD}. While the CSM is successful in describing many phenomenological aspects of quarkonia, it has become clear that it fails to provide a consistent picture of quarkonia production. Order of magnitude discrepancies have been found between CSM predictions and new measurements of ψ and Υ production at several colliders. These disagreements have called into question the validity of the CSM, and stimulated new ideas regarding quarkonia production.

Quarkonia are inherently nonrelativistic due to the large mass M_Q of the heavy quark and antiquark. Consequently, the physics of quarkonia involves a new small parameter, the velocity v of the heavy constituents inside the $Q\bar{Q}$ bound state. An effective field theory called Nonrelativistic Quantum Chromodynamics (NRQCD) has been established [1], based on a double power series expansion in the strong interaction fine structure constant $\alpha_s = g_s^2/4\pi$ and the velocity $v \sim 1/\log M_Q$. NRQCD allows for the creation at short distances of a heavy quark-antiquark pair in a color-octet configuration which later hadronized into a colorless final state quarkonia. Similar to Heavy Quark Effective Theory, NRQCD incorporates an approximate spin symmetry, which constrains various multiplet structures, transition rates, and polarizations. There have been many applications of NRQCD to quarkonia production in various high energy processes [2], but the validity of the picture still has to be verified.

NRQCD makes definite predictions of the polarization of ψ's produced in a high energy collision. Thus, one test of the color-octet picture would be observing the polarization of ψ mesons produced at the Tevatron consistent with NRQCD calculations. At large transverse momenta, quarkonia are primarily produced by gluon fragmentation [3–8]. The gluon is nearly real and transverse in the high $p_\perp$ limit, and the resulting $Q\bar{Q}[^3S_1^{(8)}]$ pair inherits this spin alignment. The long distance hadronization into a colorless ψ preserves all angular momentum information, due to the NRQCD approximate spin symmetry. Thus, ψ mesons produced at large $p_\perp$ are 100% transversely aligned [9]. Higher order α_s correction to the

polarization of ψ from gluon fragmentation have been calculated, and occur at the few percent level [10].

Gluon fragmentation is, however, only valid in the $p_\perp \gg M_Q$ limit. At low transverse momentum, large numbers of ψ's are produced via color-octet states with $L = S = 0$ and $L = S = 1$ [11,12]. Corrections to the fragmentation limit are not constrained to preserve the polarization of the ψ. Therefore, to use quarkonia polarization as a test of the color-octet mechanism, we need to investigate the spin alignment due to these states. In this paper, we will only consider the polarization of ψ' mesons. A similar analysis for other charmonia and bottomonia states is possible, but these mesons are complicated by feeddown from higher level states.

In the NRQCD formalism, the production cross section for a quarkonia state H in the reaction $A + B \rightarrow H + X$ can be written as

$$d\sigma(AB \rightarrow HX) = \sum_{ab} \int_0^1 dx_1\, dx_2\, f_{a/A}(x_1)\, f_{b/B}(x_2) \sum_n d\hat{\sigma}_{ab}[n] \langle \mathcal{O}_n^H \rangle. \tag{1}$$

The first sum in Eq. (1) is over all partons in the colliding hadrons, and the parton distribution functions are denoted by $f_{a/A}$ and $f_{b/B}$. The partonic cross section $d\hat{\sigma}_{ab}[n]$ describe the production of a quark-antiquark in a state n and can be calculated perturbatively in α_s. The NRQCD matrix elements $\langle \mathcal{O}_n^H \rangle$ parameterizes the hadronization of state n into the quarkonium state H plus light hadrons [1]. These NRQCD matrix elements contain all the nonperturbative information in the production process, and must be extracted experimentally. The order in the velocity expansion at which each of these matrix elements participates in the ψ_Q creation processes is governed by NRQCD counting rules [13].

The unpolarized cross sections for producing ψ' mesons in quark-antiquark, quark-gluon, and gluon-gluon scattering have been previously calculated up to $\mathcal{O}(\alpha_s^3 v^7)$ [11,12]. At this order, the matrix elements that appear in Eq. (1) are $\langle \mathcal{O}_1^{\psi'}(^3S_1) \rangle$, $\langle \mathcal{O}_8^{\psi'}(^3S_1) \rangle$, $\langle \mathcal{O}_8^{\psi'}(^1S_0) \rangle$, and $\langle \mathcal{O}_8^{\psi'}(^3P_0) \rangle$. The values of the color-octet matrix elements were extracted in [12,14] by fitting the magnitudes of the calculated NRQCD cross section to Tevatron data, and are

$$\langle \mathcal{O}_8^{\psi'}(^3S_1) \rangle = (4.6 \pm 1.0) \times 10^{-3} \text{GeV}^3, \tag{2a}$$

$$\frac{\langle \mathcal{O}_8^{\psi'}(^3P_0)\rangle}{M_c^2} + \frac{\langle \mathcal{O}_8^{\psi'}(^1S_0)\rangle}{3} = (5.9 \pm 1.9) \times 10^{-3}\text{GeV}^3. \tag{2b}$$

Only the linear combination of $\langle \mathcal{O}_8^{\psi'}(^1S_0)\rangle$ and $\langle \mathcal{O}_8^{\psi'}(^3P_0)\rangle$ could be extracted. The error bars are statistical and do not reflect the large systematic uncertainties in heavy quark masses, color-singlet wavefunctions, parton distribution functions and next-to-leading order corrections [14]. These matrix elements should only be considered as an order of magnitude estimate, due to the large uncertainties. Color-singlet quarkonia production is suppressed relative to the color-octet production, as can be seen in Fig. 5 of Ref. [12].

It is possible to use the results of Ref. [12] to obtain the polarization of the final state ψ' when the intermediate $Q\bar{Q}$ pair is in a $^1S_0^{(8)}$ state. For the intermediate $^3S_1^{(8)}$ or $^3P_J^{(8)}$ states, however, the analysis in Ref. [12] cannot be used to obtain a polarized cross section. As pointed out in Ref. [10], since heavy quark spin symmetry is an approximate symmetry in the NRQCD Lagrangian, L_z and S_z are good quantum numbers. Therefore, to calculate the polarization of the final state ψ' correctly, we must project the hard scattering amplitude onto states with definite L_z and S_z, square the amplitude, and then do the sum over L_z. A formalism was developed later to correctly calculate the polarization in the NRQCD framework [15]. Also, since we are interested in the polarization of the quarkonium in the hadron frame, we cannot write the amplitudes completely in terms of partonic varibles.[1] In Ref. [12], the hard scattering amplitude was projected onto states with definite JJ_z and then squared, with the polarization vectors defined in the parton frame. This will give the correct unpolarized cross section [16,15], but will not be useful in calculating the polarized cross section.

The methods used in calculating the amplitudes are similar to those described in Ref. [12], and the discussion will not be repeated here. The only difference being that we projected the amplitude onto states of definite L_z and S_z, squared, and then summed over L_z. The

---

[1]We thank M. Beneke and M. Krämer for pointing out this error in the original version of this paper.

polarization vector $\epsilon(\lambda)$ of the quarkonium state then explicitly enters the differential cross section, Eq. (1), as [14]

$$\frac{d\hat{\sigma}_{ab}^{(\lambda)}[n]}{d\hat{t}} = A_{ab}[n] + B_{ab}[n](\epsilon(\lambda) \cdot k_1)^2 + C_{ab}[n](\epsilon(\lambda) \cdot k_2)^2 + D_{ab}[n](\epsilon(\lambda) \cdot k_1)(\epsilon(\lambda) \cdot k_2), \quad (3)$$

where k_1 and k_2 are the momenta of the initial state partons a and b. The coefficients $A, \ldots, D$ are shown in the Appendix. If we sum over the polarization vector, we recover the unpolarized cross sections from Ref. [12].

The ratio of longitudinal differential cross section to the unpolarized differential cross section,

$$\xi = \frac{\sigma_L}{\sigma_T + \sigma_L}, \quad (4)$$

can be measured in $\psi' \to \ell^+\ell^-$ decay. The leptons are distributed in angle according to

$$\frac{d\Gamma(\psi' \to \ell^+\ell^-)}{d\cos\theta} \propto 1 + \alpha \cos^2\theta, \quad (5)$$

where

$$\alpha = \frac{1 - 3\xi}{1 + \xi}, \quad (6)$$

and θ denotes the angle between the lepton momentum in the ψ' rest frame and the ψ' momentum in the lab frame. In Fig. 1, we plot α for prompt ψ' production at the Tevatron.[2] Since there is only a value for the linear combination in Eq. (2b), we cannot give a definite prediction for α. Instead, the solid curve represents α when $\langle \mathcal{O}_8^{\psi'}(^3P_0) \rangle = 0$. The dashed curve illustrates α when the contribution from $\langle \mathcal{O}_8^{\psi'}(^1S_0) \rangle$ is set to zero. The shaded region illustrates the effect of the uncertainties in the matrix elements in Eq. (2).

The angular distribution approaches the transverse form $1 + \cos^2\theta$ at high $p_\perp$ as predicted by gluon fragmentation computations [9]. At low transverse momentum, the ψ' is essentially

---

[2]In this paper, MRSD0 parton distribution functions evaluated at the renormalization scale $\mu = \sqrt{p_\perp^2 + 4M_c^2}$ were used, with $M_c = 1.48$ GeV. A pseudorapidity cut of $|\eta| \leq 0.6$ was imposed.
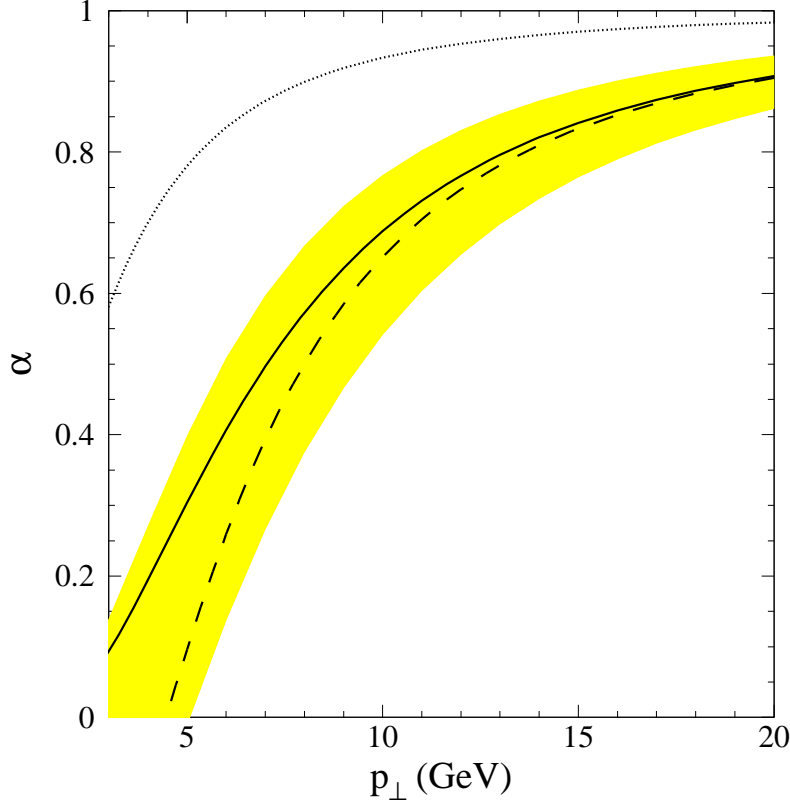
FIG. 1. Coefficient α which governs the lepton angular distribution in $\psi' \rightarrow \ell^+\ell^-$ decay plotted as a function of $p_\perp$. The solid and dashed curves illustrate α for ψ' production at the Tevatron when $\langle \mathcal{O}_8^{\psi'}(^3P_0) \rangle$ and $\langle \mathcal{O}_8^{\psi'}(^1S_0) \rangle$ respectively vanish. The shaded region shows the effect of the uncertainty in the extraction of the matrix elements. The dotted line corresponds to the lowest order, color-singlet production.

unpolarized due to $L = S = 0$ and $L = S = 1$ color-octet states. Since the two curves are similar in shape, the true value for the angular coefficient should be close to the curves shown. The effect of uncertainties in the matrix elements and higher order corrections can be qualitatively described by slight displacements of the curves in Fig. 1, without changing the asymptotic behaviors. Higher order α_s corrections, however, can change the asymptotic high $p_\perp$ behavior, but it should be a small effect [10].

Also plotted in Fig. 1 is the polarization due to the lowest order, color-singlet production, $gg \rightarrow c\bar{c}[^3S_1^{(1)}]g$. As can be seen, the qualitative shape of the color-singlet curve is similar to the color-octet curves. While higher order color-singlet corrections will modify this shape,

it is clear that by just observing the qualitative shape presented in Fig. 1 of the prompt ψ' polarization at the Tevatron will not be a clear signature for color-octet production.

ACKNOWLEDGMENTS

Functions entering into polarized cross sections:[3]

$qq \rightarrow \psi^{(\lambda)}g$:

$$A_{qq}[^3S_1^{(8)}] = \frac{4\alpha_s^3\pi^2}{81M^3\hat{s}^2} \frac{\left(4(\hat{t}^2 + \hat{u}^2) - \hat{t}\hat{u}\right)(\hat{s}^2 - 2\hat{t}\hat{u} + M^4)}{\hat{t}\hat{u}(\hat{s} - M^2)^2},$$

$$B_{qq}[^3S_1^{(8)}] = -\frac{16\alpha_s^3\pi^2}{81M\hat{s}^2} \frac{\left(4(\hat{t}^2 + \hat{u}^2) - \hat{t}\hat{u}\right)}{\hat{t}\hat{u}(\hat{s} - M^2)^2},$$

$$C_{qq}[^3S_1^{(8)}] = -\frac{16\alpha_s^3\pi^2}{81M\hat{s}^2} \frac{\left(4(\hat{t}^2 + \hat{u}^2) - \hat{t}\hat{u}\right)}{\hat{t}\hat{u}(\hat{s} - M^2)^2},$$

$$D_{qq}[^3S_1^{(8)}] = 0,$$

(A1a)

$$A_{qq}[^3P_J^{(8)}] = \frac{80\alpha_s^3\pi^2}{27M^3\hat{s}^2} \frac{\hat{s}^2 - 2\hat{t}\hat{u} + 3M^4}{\hat{s}(\hat{s} - M^2)^2},$$

$$B_{qq}[^3P_J^{(8)}] = -\frac{640\alpha_s^3\pi^2}{27M\hat{s}^2} \frac{\hat{t}\hat{u} + \hat{u}M^2 - M^4}{\hat{s}^2(\hat{s} - M^2)^3},$$

$$C_{qq}[^3P_J^{(8)}] = -\frac{640\alpha_s^3\pi^2}{27M\hat{s}^2} \frac{\hat{t}\hat{u} + \hat{t}M^2 - M^4}{\hat{s}^2(\hat{s} - M^2)^3},$$

$$D_{qq}[^3P_J^{(8)}] = \frac{640\alpha_s^3\pi^2}{27M\hat{s}^2} \frac{\hat{s}^2 + \hat{s}M^2 - 2\hat{t}\hat{u}}{\hat{s}^2(\hat{s} - M^2)^3},$$

(A1b)

$gq \rightarrow \psi^{(\lambda)}q$:

$$A_{gq}[^3S_1^{(8)}] = -\frac{\alpha_s^3\pi^2}{54M^3\hat{s}^2} \frac{\left(4(\hat{s}^2 + \hat{u}^2) - \hat{s}\hat{u}\right)(\hat{t}^2 - 2\hat{s}\hat{u} + M^4)}{\hat{s}\hat{u}(\hat{t} - M^2)^2},$$

$$B_{gq}[^3S_1^{(8)}] = \frac{2\alpha_s^3\pi^2}{27M\hat{s}^2} \frac{\left(4(\hat{s}^2 + \hat{u}^2) - \hat{s}\hat{u}\right)}{\hat{s}\hat{u}(\hat{t} - M^2)^2},$$

$$C_{gq}[^3S_1^{(8)}] = \frac{4\alpha_s^3\pi^2}{27M\hat{s}^2} \frac{\left(4(\hat{s}^2 + \hat{u}^2) - \hat{s}\hat{u}\right)}{\hat{s}\hat{u}(\hat{t} - M^2)^2},$$

$$D_{gq}[^3S_1^{(8)}] = \frac{4\alpha_s^3\pi^2}{27M\hat{s}^2} \frac{\left(4(\hat{s}^2 + \hat{u}^2) - \hat{s}\hat{u}\right)}{\hat{s}\hat{u}(\hat{t} - M^2)^2},$$

(A2a)

---

[3]The coefficients corresponding to $\langle\mathcal{O}_8^{\psi'}(^1S_0)\rangle$ production can be obtained from Ref. [12] and will not be repeated here.

$$A_{gq}[^3P_J^{(8)}] = -\frac{10\alpha_s^3\pi^2}{9M^3\hat{s}^2}\frac{\hat{t}^2 - 2\hat{s}\hat{u} + 3M^4}{\hat{t}(\hat{t} - M^2)^2},$$

$$B_{gq}[^3P_J^{(8)}] = \frac{80\alpha_s^3\pi^2}{9M\hat{s}^2}\frac{\hat{s}\hat{u} + \hat{u}M^2 - M^4}{\hat{t}^2(\hat{t} - M^2)^3}, \tag{A2b}$$

$$C_{gq}[^3P_J^{(8)}] = \frac{80\alpha_s^3\pi^2}{9M\hat{s}^2}\frac{\hat{t} + M^2}{\hat{t}^2(\hat{t} - M^2)^2},$$

$$D_{gq}[^3P_J^{(8)}] = \frac{80\alpha_s^3\pi^2}{9M\hat{s}^2}\frac{\hat{t}^2 - M^2(2\hat{s} + \hat{t})}{\hat{t}^2(\hat{t} - M^2)^3},$$

$gg \to \psi^{(\lambda)}g$:[4]

$$A_{gg}[^3S_1^{(1)}] = \frac{10\alpha_s^3\pi^2 M}{81\hat{s}^2}\frac{\hat{s}^2(\hat{s} - M^2)^2 + \hat{t}\hat{u}\,(\hat{s}\hat{t} + \hat{t}\hat{u} + \hat{u}\hat{s} - \hat{s}^2)}{(\hat{s} - M^2)^2(\hat{t} - M^2)^2(\hat{u} - M^2)^2}$$

$$B_{gg}[^3S_1^{(1)}] = -\frac{20\alpha_s^3\pi^2 M^3}{81\hat{s}^2}\frac{(\hat{s}^2 + \hat{t}^2)}{(\hat{s} - M^2)^2(\hat{t} - M^2)^2(\hat{u} - M^2)^2}, \tag{A3a}$$

$$C_{gg}[^3S_1^{(1)}] = -\frac{20\alpha_s^3\pi^2 M^3}{81\hat{s}^2}\frac{(\hat{s}^2 + \hat{u}^2)}{(\hat{s} - M^2)^2(\hat{t} - M^2)^2(\hat{u} - M^2)^2},$$

$$D_{gg}[^3S_1^{(1)}] = -\frac{40\alpha_s^3\pi^2 M^3}{81\hat{s}^2}\frac{\hat{s}^2}{(\hat{s} - M^2)^2(\hat{t} - M^2)^2(\hat{u} - M^2)^2},$$

$$A_{gg}[^3S_1^{(8)}] = \frac{\alpha_s^3\pi^2}{36M^3\hat{s}^2}\frac{\left[27(\hat{s}^2 - \hat{t}\hat{u} - M^2\hat{s}) + 19M^4\right]}{(\hat{s} - M^2)^2(\hat{t} - M^2)^2(\hat{u} - M^2)^2}$$
$$\times\left[\hat{s}^2(\hat{s} - M^2)^2 + \hat{t}\hat{u}\,(\hat{s}\hat{t} + \hat{t}\hat{u} + \hat{u}\hat{s} - \hat{s}^2)\right],$$

$$B_{gg}[^3S_1^{(8)}] = -\frac{\alpha_s^3\pi^2}{18M\hat{s}^2}\frac{\left[27(\hat{s}^2 - \hat{t}\hat{u} - M^2\hat{s}) + 19M^4\right](\hat{s}^2 + \hat{t}^2)}{(\hat{s} - M^2)^2(\hat{t} - M^2)^2(\hat{u} - M^2)^2}, \tag{A3b}$$

$$C_{gg}[^3S_1^{(8)}] = -\frac{\alpha_s^3\pi^2}{18M\hat{s}^2}\frac{\left[27(\hat{s}^2 - \hat{t}\hat{u} - M^2\hat{s}) + 19M^4\right](\hat{s}^2 + \hat{u}^2)}{(\hat{s} - M^2)^2(\hat{t} - M^2)^2(\hat{u} - M^2)^2},$$

$$D_{gg}[^3S_1^{(8)}] = -\frac{\alpha_s^3\pi^2}{9M\hat{s}^2}\frac{\left[27(\hat{s}^2 - \hat{t}\hat{u} - M^2\hat{s}) + 19M^4\right]\hat{s}^2}{(\hat{s} - M^2)^2(\hat{t} - M^2)^2(\hat{u} - M^2)^2},$$

---

[4]We have introduced the variable $\hat{z} = \sqrt{\hat{t}\hat{u}}$ to simplify some of the coefficients.

$$A_{gg}[^3P_J^{(8)}] = \frac{5\alpha_s^3\pi^2}{M^3\hat{s}^2}\Big\{M^2\hat{s}^3(\hat{s}-M^2)^3(\hat{s}^4 - 2M^2\hat{s}^3 + 7M^4\hat{s}^2 - 6M^6\hat{s} + 3M^8)$$

$$+\hat{s}^2\hat{z}^2(\hat{s}-M^2)(\hat{s}^6 - 8M^2\hat{s}^5 + 23M^4\hat{s}^4 - 50M^6\hat{s}^3 + 56M^8\hat{s}^2$$

$$-31M^{10}\hat{s} + 6M^{12})$$

$$-\hat{s}\hat{z}^4(4\hat{s}^6 - 9M^2\hat{s}^5 + 31M^4\hat{s}^4 - 71M^6\hat{s}^3 + 77M^8\hat{s}^2 - 34M^{10}\hat{s} + 6M^{12})$$

$$+\hat{z}^6(6\hat{s}^5 + 4M^2\hat{s}^4 + 20M^4\hat{s}^3 - 33M^6\hat{s}^2 + 22M^8\hat{s} - 3M^{10})$$

$$-2\hat{z}^8(2\hat{s}^3 + 2M^2\hat{s}^2 + 5M^4\hat{s} - 3M^6)$$

$$+\hat{z}^{10}(\hat{s}-M^2)\Big\}\Big/\left(\hat{s}\hat{z}^2(\hat{s}-M^2)^3(M^2s+\hat{z}^2)^3\right),$$

$$B_{gg}[^3P_J^{(8)}] = -\frac{5\alpha_s^3\pi^2}{M\hat{s}^2}\Big\{4\hat{u}^5(M^2-\hat{u})^7$$

$$-\hat{t}\hat{u}^3(M^2-\hat{u})^4(M^8 - 7M^6\hat{u} + 42M^4\hat{u}^2 - 52M^2\hat{u}^3 + 24\hat{u}^4)$$

$$+\hat{t}^2\hat{u}^2(M^2-\hat{u})^3(2M^{10} - M^8\hat{u} - 39M^6\hat{u}^2 + 152M^4\hat{u}^3 - 166M^2\hat{u}^4$$

$$+68\hat{u}^5)$$

$$-\hat{t}^3\hat{u}(M^2-\hat{u})^2(M^{12} + 9M^{10}\hat{u} + 2M^8\hat{u}^2 - 134M^6\hat{u}^3 + 361M^4\hat{u}^4$$

$$-339M^2\hat{u}^5 + 116\hat{u}^6)$$

$$+\hat{t}^4\hat{u}(M^2-\hat{u})(11M^{12} + 9M^{10}\hat{u} + 16M^8\hat{u}^2 - 274M^6\hat{u}^3 + 589M^4\hat{u}^4$$

$$-471M^2\hat{u}^5 + 128\hat{u}^6)$$

$$+\hat{t}^5(M^2-\hat{u})(4M^{12} - 51M^{10}\hat{u} + 2M^8\hat{u}^2 - 36M^6\hat{u}^3 + 282M^4\hat{u}^4$$

$$-329M^2\hat{u}^5 + 80\hat{u}^6)$$

$$-\hat{t}^6(20M^{12} - 129M^{10}\hat{u} + 94M^8\hat{u}^2 - 12M^6\hat{u}^3 + 150M^4\hat{u}^4 - 147M^2\hat{u}^5$$

$$+8\hat{u}^6)$$

$$+8\hat{t}^7(5M^{10} - 19M^8\hat{u} + 6M^6\hat{u}^2 + 6M^4\hat{u}^3 - 3M^2\hat{u}^4 + 5\hat{u}^5)$$

$$-8\hat{t}^8(5M^8 - 11M^6\hat{u} - 2M^4\hat{u}^2 + 7M^2\hat{u}^3 - 5\hat{u}^4)$$

$$+20\hat{t}^9(M^2-\hat{u})^2(M^2+\hat{u})$$

$$-4\hat{t}^{10}(M^4-\hat{u}^2)\Big\}\Big/\left(\hat{s}^2\hat{t}^2\hat{u}^2(\hat{s}-M^2)^3(\hat{t}-M^2)^3(\hat{u}-M^2)^3\right),$$

$$C_{gg}[^3P_J^{(8)}] = B_{gg}[^3P_J^{(8)}]|_{\hat{t}\leftrightarrow\hat{u}}, \tag{A3c}$$

$$D_{gg}[^3P_J^{(8)}] = \frac{10\alpha_s^3\pi^2}{M\hat{s}^2}\Big\{ 4M^2\hat{s}^6(\hat{s}-M^2)^5$$

$$-M^2\hat{s}^4\hat{z}^2(\hat{s}-M^2)^2(22\hat{s}^3-38M^2\hat{s}^2+19M^4\hat{s}-4M^6)$$

$$-2\hat{s}^3\hat{z}^4(\hat{s}^5-22M^2\hat{s}^4+62M^4\hat{s}^3-62M^6\hat{s}^2+27M^8\hat{s}-4M^{10})$$

$$+\hat{s}^2\hat{z}^6(2\hat{s}^4-17M^2\hat{s}^3+66M^4\hat{s}^2-31M^6\hat{s}+8M^8)$$

$$+2\hat{s}\hat{z}^8(3\hat{s}^3-6M^2\hat{s}^2-3M^4\hat{s}+2M^6)$$

$$-2\hat{s}\hat{z}^{10}(5\hat{s}-3M^2)+4\hat{z}^{12}\Big\}\Big/\left(\hat{s}^2\hat{z}^4(\hat{s}-M^2)^3(M^2\hat{s}+\hat{z}^2)^3\right).$$

REFERENCES

[1] G. T. Bodwin, E. Braaten and G. P. Lepage, Phys. Rev. D **51**, 1125 (1995).

[2] See E. Braaten, S. Fleming and T. C. Yuan, Ann. Rev. Nucl. Part. Sci. **46**, 197 (1996), and references therein.

[3] E. Braaten and T. C. Yuan, Phys. Rev. Lett. **71**, 1673 (1993).

[4] E. Braaten and T. C. Yuan, Phys. Rev. D **50**, 3176 (1994).

[5] E. Braaten, M. A. Doncheski, S. Fleming and M. L. Mangano, Phys. Lett. **B333**, 548 (1994).

[6] D. P. Roy and K. Sridhar, Phys. Lett. **B339**, 141 (1994).

[7] M. Cacciari and M. Greco, Phys. Rev. Lett. **73**, 1586 (1994).

[8] E. Braaten and S. Fleming, Phys. Rev. Lett. **74**, 3327 (1995).

[9] P. Cho and M. Wise, Phys. Lett. **B346**, 129 (1995).

[10] M. Beneke and I. Z. Rothstein, Phys. Lett. **B372**, 157 (1996).

[11] P. Cho and A. K. Leibovich, Phys. Rev. D **53**, 150 (1996).

[12] P. Cho and A. K. Leibovich, Phys. Rev. D **53**, 6203 (1996).

[13] G. P. Lepage, L. Magnea, C. Nakhleh, U. Magnea and K. Hornbostel, Phys. Rev. D **46**, (1992) 4052.

[14] M. Beneke and M. Krämer, Phys. Rev. D **55**, 5269 (1997).

[15] E. Braaten and Y.-Q. Chen, Phys. Rev. D **54**, 3216 (1996).

[16] M. Beneke and I. Z. Rothstein, Phys. Rev. D **54**, 2005 (1996).